Research Square

Preprints are preliminary reports that have not undergone peer review.
They should not be considered conclusive, used to inform clinical practice,
or referenced by the media as validated information.

Integrating genome-wide association study and RNA-seq to identify rhizobium inoculation-responsive genes in mung bean (Vigna radiata)

Mengjiao Li
Shanxi Agricultural University
Qing Yu
Shanxi Agricultural University
Jiawang Wei
Shanxi Agricultural University
Fei Liu
Shanxi Agricultural University
Baolong Xing
ghsxingbaolong@163.com
Shanxi Agricultural University

Research Article

Keywords: mung bean, nodulation response traits, candidate genes, genome-wide association study, transcriptome analysis

Posted Date: October 6th, 2026

DOI: https://doi.org/10.21203/rs.3.rs-10837774/v1

License: This work is licensed under a Creative Commons Attribution 4.0 International License.
Read Full License

Additional Declarations: No competing interests reported.

Abstract

Background

Mung bean (*Vigna radiata*) is an important leguminous crop capable of establishing nitrogen-fixing symbioses with rhizobia. However, nodulation responses vary significantly among mung bean genotypes, and the genetic determinants underlying this variation remain poorly understood. To address this gap, we integrated phenotypic profiling, genome-wide association study (GWAS), and transcriptome analysis (RNA-seq) to investigate the genetic basis of nodulation and growth-related responses to rhizobial inoculation and identify candidate genes associated with these traits.

Results

A panel of 218 genetically diverse mung bean genotypes was evaluated under field conditions following rhizobial inoculation across two consecutive growing seasons (2024–2025). Responses of nodulation and major agronomic traits were systematically evaluated at multiple developmental stages. Across the 20 surveyed traits, the number of genotypes exhibiting negative responses to rhizobial inoculation ranged from 39 to 155, while mean response values ranged from − 0.93 to 5.37, indicating substantial genotypic variation in rhizobial responsiveness. GWAS identified 357 significantly associated SNP loci, and 901 candidate genes were annotated within the 50-kb flanking regions of these loci. Transcriptome analysis of the contrasting genotypes LD164 and LD55 identified 561 differentially expressed genes (DEGs). Integration of GWAS and RNA-seq data prioritized 24 candidate genes encoding proteins including pectate lyase, superoxide dismutase, NRT1/PTR family transporters, and MYB transcription factors. Quantitative real-time PCR (qPCR) validation of six selected genes confirmed expression patterns consistent with the RNA-seq results.

Conclusion

These findings demonstrate substantial phenotypic variation and a complex genetic basis underlying rhizobial responses in mung bean. The identified candidate genes and associated SNP loci provide valuable resources for further functional characterization and may facilitate marker-assisted selection of mung bean varieties with improved symbiotic performance and reduced dependence on synthetic nitrogen fertilizer.

1. Introduction

Nitrogen (N) is a major nutrient required for the growth and metabolism of plants. Optimal nitrogen supply significantly enhances crop productivity. However, nitrogen overuse is a common problem in agricultural production, which increases production costs and causes significant environmental impacts, such as water eutrophication, nitrous oxide (N_2O) emissions, and soil acidification [1]. Therefore,

nitrogen fertilizer management in agroecosystems and reducing the use of synthetic nitrogen fertilizers should be important goals for sustainable food production and environmental protection.

Biological nitrogen fixation (BNF) is an efficient, cost-effective, and environmentally friendly route for nitrogen supply, which supports the productivity of global agroecosystems. BNF contributes an estimated 40–70 Tg N per year (about 87–152 Tg of urea) globally, which is around 50% of the current global annual nitrogen fertilizer production [2]. Among the various BNF systems, symbiotic nitrogen fixation between leguminous crops and rhizobia has the highest capacity for N fixation of all BNF systems and accounts for about 60% of total BNF. Therefore, understanding the molecular and physiological basis of legume–rhizobia symbiosis and the intelligent improvement of nitrogen fixation efficiency of this symbiosis has significant potential in reducing synthetic N fertilizers and in meeting national and international synthetic nitrogen fertilizer reduction targets.

Mung bean (*Vigna radiata*) is a leguminous crop and is considered to be nutritionally dense and agronomically valuable. It is also an excellent source of plant protein, micronutrients and vitamins, and contains bioactive flavonoids like vitexin and isovitexin with hypoglycemic, hypolipidemic, antipyretic and detoxifying properties. Mung bean is important for sustainable cropping systems as it has a short growth cycle, high stress tolerance, wide adaptability to the environment, and has an inherent ability to fix nitrogen in symbiosis with rhizobia bacteria. Studies have shown that its biological nitrogen fixation potential ranges from 6 to 112 kg N ha^{-1}, which can meet > 70% of its nitrogen requirement under optimum agronomic conditions [3, 4]. As a result, mung bean cultivation is important for soil fertility improvement, synthetic nitrogen fertilizer reduction, input cost saving, and regional cropping system diversification to enhance ecological resilience and agricultural sustainability.

After rhizobia infection of leguminous crops, symbiosis can provide several agronomic and physiological advantages: a decrease in the need for synthetic nitrogen fertilizers, an increase in plant growth vigor and nutrient acquisition ability, an increase in grain yield, an increase in seed quality [5], and increased tolerance to abiotic and biotic stresses [6]. However, a significant variation is observed in the results of rhizobia inoculation between crop varieties or genotypes. For example, Zhang et al. [7] found that nodule development in mung bean cultivars Pinzhong 2, Jilv 9 and Zhonglv 5 was promoted by a common rhizobia strain, but the pod number and grain yield of the former two cultivars increased significantly, whereas the latter cultivar decreased markedly. Similarly, Mott et al. [8] observed a 3.81% decrease in plant height and a 10% decrease in shoot dry biomass after inoculation. Gough et al. [9] reported a significant increase in nodule numbers and nitrogen, phosphorus, and zinc uptake, as well as an increase in aboveground biomass and yield of mung bean and a decline in aboveground phosphorus and zinc levels. Significant decreases in plant height were caused by all treatments except Bio-Gen when the same soybean cultivar was inoculated with different rhizobia strains, and HiStick® Soy application had a significant effect on nodule formation, which was further analyzed by the expression levels of symbiosis-related genes *NIC1*, *NOD21*, and *NORKb*, showing significant differences among the various strain treatments [10]. All these findings suggest that the growth-promoting ability of rhizobia is strain-genotype specific and may be very precisely regulated by the genetic basis of the host plant.

Root nodule formation and development are a highly coordinated symbiotic process which is controlled by coordinated gene regulatory networks. This involves multiple steps: molecular recognition of leguminous host by compatible rhizobia strains, infection thread initiation and elongation, cortical cell division and organogenesis to form the nodule primordium, and functional maturation of nodules, including the development of nitrogen-fixing capacity. The legume roots exude flavonoids, which serve to attract rhizobia and signal them to adhere to the root surface and trigger Nod factor synthesis. These Nod factors induce root hair curling, initiation of infection threads, and accommodation of rhizobia within the plants upon perception by plant receptors. Bacteria invade the plant, leading to the proliferation of cortical cells in the plant to form nodule primordia, which then develop into mature nitrogen-fixing organs [11, 12]. In *Medicago truncatula*, the transcription factor *MtSHR*, which is expressed in stele cells, translocates to cortical cells and cooperates with *MtSCR* to form the MtSHR–MtSCR module, which is a conserved regulatory complex that is necessary for initiation of cortical cell division in response to symbiotic signals, thus allowing nodule organogenesis and rhizobia colonization [13]. The soybean (*Glycine max*) mutants *ric-6m* and *nark* show a drastic decrease in biomass, but a significant increase in the number of nodules; the ric1a/2a mutant shows a doubling of the number of nodules, a significant increase in plant biomass, biological nitrogen fixation efficiency, photosynthetic efficiency and yield (10%–20%), and an increase in protein content (1%–2%) without a significant decrease in oil content [14]. Moreover, sucrose accumulated in the roots by rhizobia infection and translocated to infection threads is mediated by the sucrose transporter GmSWEET3c, which is directly activated by the rhizobia's symbiotic transcription factor *GmNSP1*, and whose loss of function causes a decrease in sucrose allocation in roots and leads to a significant decrease in nodule number [15]. *gmcyclops1 gmcyclops2* double mutant plants showed significantly decreased levels of *CYCLOPS* expression, which is a central regulator of legume–rhizobia symbiosis, and this double mutant also shows a significant decrease in nodule number and fresh weight, whereas the overexpression of the gene increases nodule formation and symbiotic nitrogen fixation activity [16]. Another transcription factor is Nodule Inception (NIN), which is involved in the early events of nodule formation in legumes, and *nin* mutants exhibit abortive infection, ectopic defense activation, and premature senescence of nodules [17]. CIP73 acts as a regulatory factor for NIN expression and thus on nodule formation [18]. *MaGRAS51* regulates the expression of *NIN* to modulate the number of nodules and nitrogen fixation in *Melilotus albus* under salt stress [19].

The symbiotic nitrogen fixation system of mung bean and rhizobia is significant in improving the productivity and green farming of mung bean with less fertilizer usage. However, its nitrogen fixation efficiency is significantly affected by host genotype/rhizobia strain interaction.

Although several studies have investigated the effects of rhizobia inoculation, a systematic dissection of the genetic architecture of nodulation response traits in mung bean at the population-genetic level and the identification of key regulatory genes have not been reported. To address this gap, 218 mung bean germplasm and two years of field inoculation experiments were conducted to systematically analyze the effects of rhizobia inoculation on growth and nodulation-related traits across different germplasm. To identify key candidate genes governing nodulation response traits, GWAS and RNA-seq were conducted.

This study elucidates the genetic basis of these traits and provides a theoretical basis and genetic resources for breeding high nitrogen fixation efficiency mung bean varieties.

2. Materials and Methods

2.1. Experimental Design

A total of 218 mung bean germplasm varieties, including 30 introduced varieties from abroad, were used as experimental materials. A completely randomized design with two treatments, rhizobial inoculation and non-inoculated control (water inoculation), was implemented across two consecutive field seasons. Two *Bradyrhizobium* strains (ACCC14131 and ACCC14134), which had previously been verified for symbiotic compatibility with mung bean, were cultured axenically in yeast morphology agar medium (pH 6.9) and suspended in sterile water. The two bacterial suspensions were mixed in equal volumes to obtain a final concentration of approximately OD_{600} = 0.8 immediately before inoculation. Mung bean seeds were immersed in the bacterial suspension for 30 min with gentle agitation to ensure uniform adherence of rhizobia to the seed surface. The treated seeds were then air-dried in a shaded, well-ventilated environment and sown on the same day. For the control treatment, seeds were coated with an equivalent volume of sterile water.

Field experiments were conducted over two consecutive growing seasons (2024 and 2025) at the experimental base of the High Latitude Crops Institute, Shanxi Agricultural University, Shanxi Province, China (39.92° N, 113.27° E). Each of the 218 varieties was planted in a 2 m × 5 m plot (10 m^2) with three biological replicates. At the flowering stage (FS) and seed-filling stage (SFS), measurements of the plant height (PH), nodule number (NN), root dry weight (RDW), stem dry weight (SDW), and maximum nodule diameter (ND) were carried out. At maturity, plant height (MPH), main stem diameter (MSD), number of stem branches (MSB), stem dry weight (MSDW), root dry weight (MRDW), pod number per plant (NP), seed number per plant (NS), length of the pod (PL), 100-seed weight (HSW), and yield per plant were recorded. The nodulation response trait was quantified as the inoculation-induced response, calculated as the difference between the mean value of each trait under rhizobial inoculation and that under the non-inoculated control for the same accession and replicate.

2.2. Whole-genome resequencing and SNP identification

Collection of Fresh and fully expanded leaves was carried out from individual plants at the seedling stage, and extraction of the genomic DNA was carried out while employing the cetyltrimethylammonium bromide (CTAB) method. The quality and concentration of the DNA were assessed while employing a NanoDrop spectrophotometer (Thermo Fisher Scientific, USA) and a Qubit fluorometer (Thermo Fisher Scientific, USA), respectively. Qualified genomic DNA was randomly fragmented by enzymatic digestion, followed by end repair and A-tailing. Preparation of the sequencing libraries was carried out while employing the Hieff NGS® OnePot II DNA Library Prep Kit for MGI® (Yeasen, China). DNA fragments ranging from 300 to 400 bp were selected for PCR amplification and enrichment. Sequencing was

performed using a NovaSeq X Plus platform with a paired-end 150 bp (PE150) sequencing strategy. The DNA libraries were sequenced by Genedenovo Biotechnology Co., Ltd. (Guangzhou, China). After quality filtering, the alignment of the clean reads was carried out with the mung bean reference genome (version 6.0) using BWA (version 0.7.16a-r1181). Each sample achieved an average sequencing depth of approximately 10×.

2.3. Genome-wide association study (GWAS) and population structure analysis

GWAS was performed using SNPs that met the following quality criteria: minor allele frequency (MAF) > 0.05 and missing data < 0.5 across the 218 mung bean varieties. Population structure was inferred while employing ADMIXTURE software (v1.3) [20], with the number of assumed ancestral populations (K) in the 1–9 range. Determination of the optimal K value was carried out based on the minimum cross-validation (CV) error. GCTA software (v1.93.2) was employed for performing Principal component analysis (PCA) [21]. Linkage disequilibrium (LD) decay was analyzed employing PopLDdecay software (v3.41) [22]. The LD magnitude (r^2) between pairwise SNP markers was calculated and plotted against the corresponding genetic distance to generate the LD decay curve.

Association analyses between SNP markers and phenotypic traits were performed using the mixed linear model (MLM) implemented in GEMMA software (v0.98.1) [23]. The significance threshold was set at $-\log_{10}(P) > 5.00$ [24]. Retrieval of the genes located within 50 kb upstream or downstream of significant SNPs was carried out, and these were considered candidate genes.

2.4. RNA-seq, transcription analysis and quantitative real-time PCR (qPCR)

Mung bean varieties exhibiting statistically significant differences in nodule number between rhizobial-inoculated and non-inoculated treatments were selected for transcriptome analysis. A total of 120 healthy, plump, and uniformly sized seeds were sown in plastic pots (10 cm in diameter × 12 cm in depth), each containing sterilized substrate consisting of sand and soil at a 2:1 (v/v) ratio. The substrate was sterilized by autoclaving at 121°C for 2 h. For each variety, 20 pots were prepared, with three seedlings grown per pot. Plants were maintained in a controlled-environment incubator at 28°C under a 16 h light/8 h dark photoperiod. Experimental and control groups were established in parallel. The experimental group received a uniform application of rhizobial suspension, whereas the control group received an equivalent volume of sterile distilled water. At the onset of visible root nodule formation, root tissues were harvested. The roots were gently rinsed to remove adhering substrate, surface-dried, followed by immediate wrapping in aluminum foil, flash-freezing in liquid nitrogen, and storing at − 80°C until further analysis. Subsets of the collected samples were used for transcriptome sequencing by Shanghai OE Biotech Co., Ltd. and subsequent qPCR validation.

Extraction of total RNA, synthesis of first-strand cDNA, and qPCR were carried out as previously described [25]. The primers employed for qPCR are listed in Supplementary Table S1. Relative gene

expression levels were normalized to the reference gene *VrActin* and calculated while employing the method of $2^{-\Delta Ct}$. One-way analysis of variance (ANOVA) was performed while employing IBM SPSS Statistics 22, followed by Fisher's least significant difference (LSD) post hoc test, with $P < 0.05$ considered statistically significant. Each qPCR assay included three technical replicates per sample and three independent biological replicates per treatment.

3. Results

3.1. Population structure and linkage disequilibrium decay of 218 genotypes

In total, 1,095,000 SNPs and 159,000 insertion–deletion (indel) variants were found in the 218 mung bean varieties. The heatmap of the genetic relationship matrix (Fig. 1) showed that most of the values are below 1, which represents low genomic similarity between the genotype pairs. PCA showed that PC1 explained 5.77% of the total genetic variability, with most of the variation being spread over other principal components. Structure analysis of the genotypes revealed that the optimal number of subpopulations was K = 6, with the six subpopulations containing 33, 45, 26, 29, 56, and 29 genotypes, respectively. LD decay analysis showed that the physical distance at which the squared correlation coefficient (r^2) declined to half its maximum value was 116.5 kb.

3.2. Phenotypic analysis of nodulation response traits

Phenotypic data were systematically sampled at various stages of plant growth and various tissue types for two growth seasons. There was significant variation among the 218 mung bean varieties in 20 nodulation response traits (Fig. 2). The mean of the responses of the different growth stages on the investigated traits ranged from − 0.93 to 5.37 (Table 1). Five traits exhibited negative mean responses, four of which were maturity-stage traits, including MPH, HSW, PL, and NS. The traits with the widest ranges between minimum and maximum response values were FSNN (− 20.33 to 46.17), SFSNN (− 26.83 to 41.50), SFSSDW (− 22.05 to 41.05), and NP (− 29.20 to 46.20). Nodule number at the flowering and seed-filling stages exhibited pronounced positive skewness (2.49 and 1.74, respectively) and high kurtosis (10.42 and 7.93, respectively). Among all traits, NS had the highest proportion of varieties showing negative responses to rhizobial inoculation (155 of 218), followed by HSW (152 of 218). Nodule number at the seed-filling and flowering stages showed the lowest proportions of negative responses, with 39 and 40 varieties, respectively. Broad-sense heritability estimates ranged from 0.07% to 33.51% among the 20 traits, with SFSSDW showing the highest estimated heritability and SFSND showing the lowest, suggesting more genetic contribution to the variation in SFSSDW and a larger environmental contribution to the variation in SFSND. Shapiro–Wilk tests indicated that 12 of the 20 traits did not significantly deviate from a normal distribution ($P > 0.05$). Significant differences among the six genetic subgroups were observed for all 20 traits (Figure S1).

Table 1
Descriptive statistics of 20 nodulation response traits across 218 mung bean genotypes.

Traits	Max	Min	Average	Skewness	Kurtosis	Shapiro-wilk value	H^2
FSPH	13.42	-10.42	1.43	-0.02	0.45	0.28	14.78
FSNN	46.17	-20.33	3.92	2.49	10.42	0.00	14.14
FSND	6.19	-5.19	1.06	-0.21	-0.27	0.16	3.72
FSRDW	0.99	-0.32	0.20	0.53	0.32	0.00	4.91
FSSDW	15.43	-9.29	3.22	-0.06	-0.17	0.47	19.43
SFSPH	16.92	-10.83	-0.61	0.36	0.82	0.03	15.88
SFSNN	41.50	-26.83	4.29	1.74	7.93	0.00	3.36
SFSND	6.33	-5.71	1.39	-0.26	-0.45	0.07	0.07
SFSRDW	1.52	-0.73	0.20	0.23	0.05	0.29	6.56
SFSSDW	41.05	-22.05	5.37	-0.02	0.25	0.40	33.51
MPH	9.30	-15.90	-0.93	-0.70	1.20	0.00	1.22
MSD	2.58	-2.09	0.11	0.06	-0.27	0.81	23.73
MSB	2.80	-1.60	0.50	-0.05	0.35	0.58	12.21
Yield	12.75	-9.23	0.88	0.20	-0.38	0.22	6.97
MRDW	1.52	-0.85	0.09	0.56	0.54	0.01	3.42
MSDW	24.45	-25.98	0.47	0.16	0.36	0.55	17.24
HSW	1.07	-1.49	-0.16	0.14	1.14	0.01	1.79
NP	46.20	-29.20	4.47	0.28	0.30	0.25	14.44
PL	1.22	-1.63	-0.07	-0.10	1.01	0.00	13.10
NS	1.76	-1.94	-0.32	0.01	0.81	0.05	29.42

Table 2
Candidate genes identified through integrated GWAS and RNA-seq analysis.

Gene_id	Regulation	Description
Vradi01g07160	Down	Dehydration-responsive element-binding protein 1D
Vradi02g08940	Down	Probable O-methyltransferase 3
Vradi02g09790	Down	Callose synthase 3
Vradi02g11650	Up	Receptor-like protein kinase
Vradi05g05860	Up	Probable pectate lyase 18
Vradi05g10790	Up	Phosphopantothenate–cysteine ligase 2
Vradi06g03450	Up	Polygalacturonase-1 non-catalytic subunit beta
Vradi06g11750	Up	Stearoyl-[acyl-carrier-protein] 9-desaturase 6, chloroplastic
Vradi06g12140	Up	Clathrin heavy chain 1
Vradi07g26450	Down	Oligopeptide transporter 3
Vradi07g26540	Down	CASP-like protein 2B1
Vradi07g27690	Up	Kinesin-like protein KIN-14C
Vradi07g27900	Up	Endoglucanase 8
Vradi08g10970	Down	Transcription factor MYB78
Vradi08g15680	Up	Superoxide dismutase [Fe], chloroplastic
Vradi08g20580	Up	Heavy metal-associated isoprenylated plant protein 37
Vradi08g20690	Down	Probable ribose-5-phosphate isomerase 2
Vradi09g04830	Up	(+)-neomenthol dehydrogenase
Vradi09g08870	Up	Protein GAMETE EXPRESSED 1
Vradi10g00970	Up	Uncharacterized protein
Vradi10g05710	Up	Flavonoid 3',5'-hydroxylase 1
Vradi10g11820	Up	Probably inactive leucine-rich repeat receptor-like protein kinase At5g48380
Vradi10g12830	Up	Separase
Vradi11g03570	Up	Protein NRT1/ PTR FAMILY 7.3

Across the 20 traits, responses to rhizobial inoculation showed varying degrees of correlation, with most trait pairs exhibiting positive correlations (Fig. 2). The response of NP showed a strong positive correlation with yield, indicating that genotypes with more changes in NP tended to exhibit more

pronounced changes in yield following rhizobial inoculation. Among the 20 traits, MPH, MSDW, and MRDW showed the highest numbers of positive correlations with other response traits, with 14, 13, and 13 significant positive correlations, respectively, suggesting that these growth-related traits were broadly associated with other phenotypic responses to rhizobial inoculation. HSW showed only four negative correlations with other response traits, including highly significant negative correlations with FSND and SFSND and a significant negative correlation with SFSNN. These associations suggest a potential trade-off between seed size-related responses and nodule development under rhizobial inoculation.

3.3. GWAS and identification of candidate genes

GWAS was performed for 20 nodulation response traits and identified 357 significantly associated SNP loci distributed across all 11 chromosomes. Chromosome 7 harbored the largest number of significant loci (99), followed by chromosome 6 (73), whereas chromosomes 4 (6 loci), 3 (7 loci), and 11 (9 loci) contained fewer significant associations. The phenotypic variance explained (PVE) by individual significant SNPs ranged from 4.3% to 46.3%. Among these loci, 9_17107663 and 9_6943935 showed the highest PVE values, at 46.3% and 45.7%, respectively, and both were associated with SFSNN. Eight loci had PVE values below 5%, including five loci on chromosome 1, one on chromosome 5, and two on chromosome 11. These loci were associated with MPH and MSD, with locus 11_14574901 showing the lowest PVE and being associated with MSD. Among the 20 traits, MSD was associated with the largest number of significant SNP loci (53), followed by SFSNN (52), whereas Yield showed the fewest associations (1 locus), followed by FSPH (2 loci). Locus 11_15912172 was simultaneously associated with MPH and MSDW, whereas the remaining significant loci were associated with only one trait (Fig. 3).

Candidate genes were identified by searching the 50-kb upstream and downstream regions flanking each of the 357 significant SNP loci, resulting in 901 candidate genes. Gene IDs and functional annotations are provided in Table S1. These candidate genes encoded proteins with diverse molecular functions, including ABC transporters, potassium transporters, NRT1/PTR nitrate transporters, ethylene-responsive transcription factors, MYB, NAC, TCP, and bHLH transcription factors, glycosyltransferases, pectinesterases, sulfotransferases, calmodulins, and pathogenesis-related proteins. Among these candidates, 55 genes were associated with two traits. Gene Ontology (GO) enrichment analysis showed that the candidate genes were predominantly associated with molecular functions related to binding and catalytic activity, localized mainly to cellular components such as the cell, organelle, and membrane, and involved in biological processes including cellular processes, metabolic processes, and single-organism processes. KEGG (Kyoto Encyclopedia of Genes and Genomes) pathway enrichment analysis indicated significant enrichment in pathways including fatty acid degradation, diterpenoid biosynthesis, selenocompound metabolism, monoterpenoid biosynthesis, and flavonoid biosynthesis (Figure S2).

3.4. RNA-seq analysis and identification of DEGs

Nodulation phenotypes were evaluated in the selected mung bean genotypes following rhizobial inoculation. Under the non-inoculated control condition, LD164 did not form nodules at either the flowering or seed-filling stage. Following rhizobial inoculation, nodule numbers in LD164 increased to 32

and 33 at the flowering and seed-filling stages, respectively. LD55 produced 1 and 0 nodules at the flowering and seed-filling stages, respectively, under the non-inoculated control condition, whereas rhizobial inoculation resulted in 0 and 4 nodules at the corresponding stages. Based on the contrasting nodulation responses of LD55 and LD164, these two genotypes were selected for transcriptome analysis. Root tissues were collected at the early nodule formation stage, approximately 30 days after planting, for RNA-seq. Differential expression analysis identified 561 significantly DEGs, including 339 upregulated and 222 downregulated genes. GO enrichment analysis showed that the DEGs were significantly associated with biological processes, including cellular processes, single-organism processes, and metabolic processes; cellular components, including the cell, cell part, membrane, and organelle; and molecular functions, including binding and catalytic activity. KEGG pathway enrichment analysis indicated that the DEGs were mainly enriched in pathways related to the biosynthesis of secondary metabolites, carotenoid biosynthesis, flavonoid biosynthesis, plant hormone signal transduction, and peroxisome (Fig. 4).

3.5. Candidate gene screening by integration of GWAS and RNA-seq

Integration of the GWAS and RNA-seq datasets identified 24 candidate genes that were both located within GWAS-associated regions and differentially expressed under rhizobial inoculation. These genes were distributed across nine chromosomes, with no candidates identified on chromosomes 3 and 4. Of the 24 candidate genes, 17 were found upregulated, and 7 were found downregulated. The upregulated genes encoded proteins including pectate lyase, superoxide dismutase, and NRT1/PTR family proteins, whereas the downregulated genes encoded proteins including callose synthase, oligopeptide transporters, and MYB transcription factors. To further validate the RNA-seq results, six candidate genes were selected for qPCR analysis. Consistent with the RNA-seq results, qPCR analysis showed significant downregulation of *Vradi01g07160*, *Vradi02g08940*, and *Vradi08g10970* and significant upregulation of *Vradi05g10790*, *Vradi09g04830*, and *Vradi11g03570* in LD164 relative to LD55 (Fig. 5). These results were consistent with the transcriptomic data and supported the reliability of the RNA-seq analysis, while identifying these genes as potential candidates involved in the nodulation response of mung bean.

4. Discussion

Nitrogen (N_2) is the most abundant element in the atmosphere; however, most plants cannot directly assimilate atmospheric N_2 and therefore depend heavily on chemical nitrogen fertilizers to meet their nitrogen requirements. Symbiotic nitrogen fixation, including the mutualistic relationship between leguminous crops and rhizobia, is a process in which biological N_2 fixation can take place to produce ammonia that is taken up by the host plant. This process provides an alternative green technology to chemical nitrogen fertilization, reducing the overuse of chemical nitrogen fertilizers and associated environmental impacts. However, genotype-specific responses to rhizobia inoculation are pronounced across legume species. In this study, among 20 traits surveyed, the number of genotypes with negative

responses varied from 39 to 155, and the mean response varied from − 0.93 to 5.37 (Table 1). From these results, it is clear that the effect of rhizobia inoculation is not consistent across all genotypes and can negatively impact the growth and development of some genotypes. Consistent with this, Delie et al. [26] reported a significant rhizobia-induced increase in the number of branches, number of pods, biomass, grain yield, and harvest index in mung bean varieties Rasa and Boreda, while variety Shewarobit exhibited negative responses in these traits. Szczerba et al. [10] observed that inoculation with HiStick® Soy significantly reduced root nodule number and plant height. The results indicate that there is strain–genotype specificity in the symbiotic efficacy of rhizobia in leguminous crops. However, the negative responses observed in certain varieties and traits after rhizobia inoculation may be due to several factors such as environmental stress, variety–strain compatibility, and disruption of native phytohormone signaling networks. Symbiotic bacteria can activate defense-related MAPK signaling cascades that promote the expression of defense and stress-responsive genes, which have a negative effect on early nodulation, significantly reducing symbiotic efficiency and thus leading to negative inoculation effects [27]. Further disruption of the precise equilibrium of communication between phytohormone signaling and immune response (such as cytokinins, auxin, jasmonic acid, ethylene, and abscisic acid) may result in abnormal nodule formation or failure of nitrogen-fixing function [28, 29]. A strong positive correlation between the response values of NP, NS, and yield was observed (Fig. 2), indicating that the yield modulation mediated by inoculation is mostly associated with pod number and seed number. The response value of hundred-seed weight showed significant negative correlations with FSND, SFSND, and SFSNN. These associations may reflect competition for host carbon resources between nodules and reproductive tissues. Symbiotic N_2 fixation imposes significant energetic costs on the host because nodule maintenance and nitrogenase activity require carbon inputs. Excessive nodule development may therefore increase carbon demand and potentially alter carbon allocation to aboveground tissues and developing seeds, which could affect biomass accumulation and yield [14, 30].

Overall, 357 SNP loci were found to be significantly associated by GWAS. About 48% of these loci were mapped to chromosomes 6 and 7, suggesting the presence of possible genomic hotspots in nodulation regulation in mung bean. A total of 901 candidate genes were annotated in the 50-kb flanking regions of each significant locus. Functional enrichment analysis revealed their involvement in transcriptional regulation, transport, and signal transduction. KEGG pathway enrichment analysis further demonstrated significant enrichment of metabolic pathways, including 'fatty acid degradation', 'terpenoid backbone biosynthesis', and 'flavonoid biosynthesis'. Flavonoids are important symbiotic signaling molecules that activate the rhizobia transcriptional regulator NodD and promote Nod factor biosynthesis, rhizobia infection, and root colonization. Previous research has shown that the protein SPX1/3-PHR2 network [31], the network GmUVR8-GmSTF3 [32], as well as isoflavone reductase proteins [33], are involved in the biosynthesis of flavonoids, which in turn affects nodulation of leguminous crops. To further select the most important candidates with biological credibility, our study adopted the strategy of combining RNA-seq data from rhizobia inoculation and control, resulting in 24 genes that were significantly differentially expressed and related to nodulation performance. These include genes coding for proteins with various

functions, such as pectate lyase, superoxide dismutase, nitrate transporter (NRT1/PTR family), and MYB transcription factor.

The candidate genes included multiple members of the MYB, NAC, TCP, and bHLH transcription factor families. The MYB family is one of the largest transcription factor families in plants and participates in diverse developmental processes and responses to environmental stress. In soybean, RNAi-mediated knockdown of the MYB gene *CND* reduced nodule number by 40%, while producing a marginal increase in nodule size [34]. In *Medicago truncatula*, *MtMYB40* is rapidly and strongly induced in root hairs and cortical cells following rhizobial inoculation and directly activates the flavonoid biosynthesis genes *CHS1* and *ChOMT1*. The *mtmyb40* mutant exhibits reduced infection thread formation and nodule number, particularly under low rhizobial inoculum conditions. Genetic interaction analyses further showed that MtMYB40 associates with the GRAS-domain protein MtNSP2 to co-activate *ChOMT1* expression, promoting nodulation [35]. In this study, nine MYB transcription factor genes were identified among the GWAS-derived candidates. *Vradi08g10970* showed significantly higher expression in LD55 than in LD164, suggesting that its expression is associated with the contrasting nodulation phenotypes of these genotypes and warrants further investigation as a potential regulator of nodulation.

Salt stress also negatively affects the growth of the legumes and the interaction between the rhizobia and roots. For example, *GmERF13* was found to be salt stress-induced, and the nodule number of the *GmERF13* mutant was significantly higher than that of the wild type under salt stress, suggesting that loss of *GmERF13* improved the nodulation inhibition caused by salt stress [36]. Similarly, the overexpression of *GmNAC181* led to the up-regulation of *GmNINa* and an increase in the number of nodules, particularly under salt stress conditions. *GmNAC181* is strongly induced under these conditions, and transgenic plants maintain higher nodulation capacity [37]. Some NAC transcription factors are also involved in nodule senescence. *LjNAC094* accelerates nodule aging in *Lotus japonicus* by upregulating the expression of senescence-associated genes that are responsive to nitrate [38], and *GmNAC039* and *GmNAC018* induce senescence of soybean nodules by transcriptional activation of a cytochrome P450 gene, *GmCYP* [39]. Three members of each ERF and NAC transcription factor family were identified as significantly associated with nodulating traits in GWAS. They may be involved in nodule initiation, development, and stress-responsive regulation, which need further functional validation.

ATP-binding cassette (ABC) transporters use energy derived from ATP hydrolysis to transport diverse substrates across cellular membranes, including phytohormones such as abscisic acid (ABA), cytokinins, and auxins. In *Medicago truncatula*, MtABCG20 functions as an ABA exporter and is expressed in both roots and nodules. The *mtabcg20* mutant demonstrates a significant reduction in lateral root number under drought stress but an 18% increase in nodule number relative to the wild type [40]. MtABCG40, a cytokinin-associated transporter predominantly expressed in roots, is transcriptionally induced by nitrogen deficiency and exogenous cytokinin. Under low-nitrogen conditions, MtABCG40 mediates cytokinin efflux from the xylem into surrounding cortical tissues, affecting lateral root density and nodule formation and contributing to root system architecture [41]. Five ABC transporter genes were identified among the GWAS-derived candidates in this study. These genes may contribute to mung bean

nodulation through effects on phytohormone transport and signaling, particularly pathways involving ABA and cytokinins. However, their specific functions in mung bean nodulation require experimental validation.

Nitrate uptake from soil is primarily mediated by two functionally distinct transporter systems: the low-affinity transport system mediated by the NPF family and the high-affinity transport system mediated mainly by the NRT2 family. In *Lotus japonicus*, *LjNPF8.6* is highly expressed in root nodules, and its mutant exhibits impaired nitrogen fixation capacity and increased superoxide accumulation in nodules [42]. *LjNPF3.1* is strongly expressed in mature nodules, and the *ljnpf3.1* mutant consistently shows reduced nodule fresh weight and acetylene reduction activity (ARA), regardless of the nitrogen supply level [43]. High nitrate concentrations generally inhibit nodulation, whereas low nitrate concentrations have limited effects on nodule formation [44]. Under low-nitrogen hydroponic conditions, the *ljnrt2.4* mutant exhibits a 50% reduction in nodule ARA, severely impaired nitrogen fixation, a 38%–75% reduction in nodule nitrate content, and pronounced symptoms of nitrogen deficiency, including stunted shoot growth and chlorosis [45]. LjNLP1 acts as a transcriptional activator of *LjNRT2.1* and regulates nitrate acquisition. Under high-nitrate conditions, nodule growth is inhibited in wild-type plants, whereas this inhibitory effect is largely abolished in the *ljnrt2.1* mutant. As a positive regulator of nodulation, LjNIN can counteract the induction of *LjNRT2.1* expression by LjNLP1, contributing to the regulation of nitrate uptake during nodulation [46]. In this study, one NRT2 and three NPF family genes were identified among the GWAS-derived candidates. *Vradi11g03570* showed higher expression in the high-nodulating genotype LD164 than in LD55, suggesting that its transcriptional activity may be associated with nodule development and nitrogen acquisition.

Pectate lyases play important roles in rhizobial penetration of the plant cell wall and initiation of infection thread formation. The *ljnpl* mutant exhibits a significant reduction in total infection thread number and abnormal infection events in root tissues; most resulting nodules are small and white, with only a small proportion developing into larger, partially pink nodules [47]. In soybean, *GmNPLa* is specifically induced in root hairs following rhizobial inoculation. Its overexpression increases infection thread formation by 96%, accompanied by increases in total nodule number and lateral root nodule density, whereas the *gmnpla* loss-of-function mutant exhibits significant reductions in infection thread number, lateral root number, and nodule number [48]. In this study, the orthologous gene *Vradi01g07160* showed higher expression in the low-nodulating genotype LD55 than in LD164. This expression pattern suggests that *Vradi01g07160* may participate in the early rhizobial infection process; however, its specific role in infection thread development and nodulation in mung bean requires functional validation.

Callose deposition and callose synthase activity are important components of plant immune responses. Following pathogen invasion, rapid callose deposition at infection sites contributes to cell wall reinforcement and forms a physical barrier against pathogen penetration [49]. Reactive oxygen species (ROS) also function as signaling molecules in plant growth, development, and stress responses and participate in multiple stages of legume–rhizobia symbiosis, from infection to nodule senescence, with superoxide dismutase (SOD) playing an important role in maintaining ROS homeostasis [50]. In this

study, callose synthase expression was significantly lower in the high-nodulating genotype LD164 than in LD55. This expression pattern may reflect reduced activation of callose-associated defense responses during rhizobial infection, potentially facilitating bacterial entry and nodule formation. On the contrary, the higher expression of Fe-superoxide dismutase in LD164 may indicate enhanced ROS-scavenging capacity and control of oxidative stress during early symbiotic development.

While this study has identified a set of significant candidate genes involved in nodulation responses in mung bean using GWAS and transcriptome analysis, some limitations remain. First, only two rhizobia strains were used for inoculation experiments, and it is well documented that there is variation among rhizobia strains in infection efficiency and host specificity; therefore, the validity and generalizability of the identified candidates to other strain–host combinations remain to be experimentally validated. Second, transcriptomic data were obtained from root tissues collected under controlled pot-based conditions; gene expression patterns observed here may be incomplete in the sense that they do not fully reflect those occurring in the field, where features like the complexity of the soil microbiome, the spatial variability of nutrients, and abiotic stress factors can have a strong impact on the symbiotic performance. Third, the biological activities and molecular mechanisms of the candidate genes must be validated using stable genetic transformation together with detailed molecular phenotyping. Future research should be directed towards: (1) increasing the diversity of rhizobia strains to evaluate the stability of expression of the candidate genes and to quantify the quantitative contribution of these genes in nitrogen fixation efficiency in different strain–genotype combinations; (2) future targeted functional characterization of the candidate genes including CRISPR/Cas9-mediated knockout, RNAi knockdown, and overexpression in transgenic mung bean lines to delineate the precise role of the core candidates in infection thread formation, nodule organogenesis, and symbiotic nitrogen fixation; and (3) use of natural population panels for haplotype-based association mapping for finding elite allelic variants of these candidate genes and development of tightly linked SNP markers to allow direct deployment in marker-assisted selection for high nitrogen-fixing mung bean cultivars. In summary, this study has contributed significantly to the groundwork of the genetic improvement of symbiotic N_2 fixation of the mung bean–rhizobia complex, and the candidate genes and SNP markers identified in the study will prove to be valuable molecular tools for the green and high-efficiency breeding of mung bean.

5. Conclusions

In this study, the genetic architecture of rhizobium-induced nodulation and growth-related traits in mung bean was systematically investigated by combining a two-year field phenotyping experiment for 218 mung bean genotypes with GWAS and RNA-seq. Phenotypic evaluation after rhizobia inoculation showed that 20 traits showed significant inter-varietal variation ranging from − 0.93 to 5.37, with mean response values, indicating significant genotype-by-rhizobia interaction for symbiotic growth promotion. Pod number and seed number at the mature stage were found to be the most important traits affecting yield response amongst these. There was a highly positive correlation between hundred-seed weight response and nodule number response and nodule size response, indicating coordinated regulation of reproductive output with symbiotic capacity. GWAS identified 357 significantly associated SNP loci and

901 positional candidate genes that were functionally enriched in nodulation signaling and energy metabolism pathways, such as flavonoid biosynthesis, terpenoid backbone biosynthesis, and fatty acid degradation pathways. For root-based tissues, RNA-seq analysis of root tissues of the extreme-phenotype genotypes identified 561 DEGs with enrichment in pathways such as flavonoid biosynthesis, plant hormone signal transduction, and peroxisomal metabolism. Integrative GWAS and RNA-seq prioritized 24 candidate genes that were significantly associated with nodulation traits and whose expression levels differed significantly under rhizobia inoculation. The genes are likely to play key roles in symbiotic functions, such as infection thread elongation, regulation of ROS homeostasis, nitrogen-responsive signaling, and fine-tuned modulation of defense responses. This study contributes valuable genomic tools to better understand the molecular mechanisms that regulate mung bean–rhizobia symbiosis for nitrogen fixation, and the identified candidate genes and SNP markers can serve as theoretical resources for marker-assisted selection to breed mung bean varieties with high nitrogen fixation efficiency.

Declarations

Ethics approval and consent to participate

Not applicable

Consent for publication

Not applicable.

Availability of data and materials

All relevant data can be found within the manuscript and its supplementary data published online.

Competing interests

The authors declare that they have no competing interests.

Funding

This research was funded by the National Key Research and Development Program of China (2021YFD1600602-07), the China Agriculture Research System of MOF and MARA (CARS-08-Z5) and Shanxi Province Major Science and Technology Special Project Plan (202301140601016).

Authors' contributions

BLX conceived and designed the experiment, participated in the revision of the paper. MJL collated and analyzed the experimental data, wrote the first draft, plotted the graphs, and participated in the discussion of the results and revision of the paper. QY and JWW collected and processed materials. FL

was involved in revising the thesis. All authors reviewed the results and approved the final version of the manuscript.

Acknowledgements

Not applicable.

References

1. Sutton MA, Oenema O, Erisman JW, Leip A, van Grinsven H, Winiwarter W. Too much of a good thing. Nature. 2011;472(7342):159–61. https://doi.org/10.1038/472159a.
2. Goyal RK, Schmidt MA, Hynes MF. Molecular biology in the improvement of biological nitrogen fixation by rhizobia and extending the scope to cereals. Microorganisms. 2021;9(1):125. https://doi.org/10.3390/microorganisms9010125.
3. Ji XL, Wang P, He XL, Jiang YZ. Determining nitrogen accumulation and nitrogen use efficiency of mung bean with organic nitrogen and ^{15}N-labeled chemical fertilizer. Commun Soil Sci Plant Anal. 2022;53(10):1235–45. https://doi.org/10.1080/00103624.2022.2046024.
4. Shah Z, Shah SH, Peoples MB, Schwenke GD, Herridge DF. Crop residue and fertiliser N effects on nitrogen fixation and yields of legume–cereal rotations and soil organic fertility. Field Crops Res. 2003;83(1):1–11. https://doi.org/10.1016/S0378-4290(03)00005-4.
5. Gough EC, Owen KJ, Zwart RS, Thompson JP. Arbuscular mycorrhizal fungi acted synergistically with *Bradyrhizobium* sp. to improve nodulation, nitrogen fixation, plant growth and seed yield of mung bean (*Vigna radiata*) but increased the population density of the root-lesion nematode *Pratylenchus thornei*. Plant Soil. 2021;465(1-2):431–52. https://doi.org/10.1007/s11104-021-05007-7.
6. Wang T, Wu F, Liu HW, Zhang XY, Zhou YH, Zhang SL, et al. Symbiotic nodulation enhances legume tolerance to abiotic stresses: Mechanisms and perspectives. Plant Cell Environ. 2026;49(7):4513–23. https://doi.org/10.1111/pce.70207.
7. Zhang XX, Ma XT, Cao YH, Tang X, Jiang XY, Jiang RB. Impacts of rhizobial inoculation on plant growth and yield traits of green bean (*Vigna radiata*). Soil Fertil Sci China. 2012(6):70–3.
8. Mott J, Abaye O, Reiter M, Maguire R. Evaluating effects of *Bradyrhizobium* and arbuscular mycorrhizal fungi inoculation on yield components of mung bean (*Vigna radiata* (L.) Wilczek) and nitrogen fixation. Agronomy-Basel. 2022;12(10):2358. https://doi.org/10.3390/agronomy12102358.
9. Gough EC, Owen KJ, Zwart RS, Thompson JP. The role of nutrients underlying interactions among root-nodule bacteria (*Bradyrhizobium* sp.), arbuscular mycorrhizal fungi (*Funneliformis mosseae*) and root-lesion nematodes (*Pratylenchus thornei*) in nitrogen fixation and growth of mung bean (*Vigna radiata*). Plant Soil. 2022;472(1-2):421–49. https://doi.org/10.1007/s11104-021-05254-8.
10. Szczerba A, Plazek A, Kopec P, Wojcik-Jagla M, Dubert F. Effect of different Bradyrhizobium japonicum inoculants on physiological and agronomic traits of soybean (*Glycine max* (L.) Merr.)

associated with different expression of nodulation genes. BMC Plant Biol. 2024;24(1):1201. https://doi.org/10.1186/s12870-024-05911-x.

11. Yang J, Lan LY, Jin Y, Yu N, Wang D, Wang ET. Mechanisms underlying legume-rhizobium symbioses. J Integr Plant Biol. 2022;64(2):244–67. https://doi.org/10.1111/jipb.13207.
12. Wang DP, Dong WT, Murray J, Wang ET. Innovation and appropriation in mycorrhizal and rhizobial Symbioses. Plant Cell. 2022;34(5):1573–99. https://doi.org/10.1093/plcell/koac039.
13. Dong WT, Zhu YY, Chang HZ, Wang CH, Yang J, Shi JC, et al. An SHR–SCR module specifies legume cortical cell fate to enable nodulation. Nature. 2021;589(7843):586–90. https://doi.org/10.1038/s41586-020-3016-z.
14. Zhong XB, Wang J, Shi XL, Bai MY, Yuan CC, Cai CL, et al. Genetically optimizing soybean nodulation improves yield and protein content. Nat Plants. 2024;10(5):736–42. https://doi.org/10.1038/s41477-024-01696-x.
15. Chen K, Wang XD, Pang RQ, Chen L, Chen JH, Ren ZY, et al. The sucrose transporter GmSWEET3c drives soybean nodulation by regulating root sucrose allocation. Curr Biol. 2025;35(17):4121–34.e4. https://doi.org/10.1016/j.cub.2025.07.032.
16. Lei YT, Liu Z, Chen Q, Wu XT, Li M, Liu FL, et al. The *GmCYCLOPS* paralogs regulate soybean nodulation and exhibit signatures during domestication. Plant Sci. 2026;371:113287. https://doi.org/10.1016/j.plantsci.2026.113287.
17. Liu JY, Rasing M, Zeng T, Klein J, Kulikova O, Bisseling T. NIN is essential for development of symbiosomes, suppression of defence and premature senescence in *Medicago truncatula* nodules. New Phytol. 2021;230(1):290–303. https://doi.org/10.1111/nph.17215.
18. Li H, Ou YJ, Zhang JD, Xiao AF, Zhang ZM, Cao YR, et al. *Lotus japonicus* CIP73 functions as a transcriptional repressor to inhibit *Nodule Inception* gene expression in nodule symbiosis. Plant Soil. 2025;513(2):2789–806. https://doi.org/10.1007/s11104-025-07349-y.
19. Wang SS, Xiao YY, Ao B, Yan Q, Wu F, Han YY, et al. GRAS51 promotes legume symbiotic nitrogen fixation and salt tolerance of nodulation by directly regulating *NIN* expression. Plant Physiol. 2025;199(3):kiaf571. https://doi.org/10.1093/plphys/kiaf571.
20. Alexander DH, Novembre J, Lange K. Fast model-based estimation of ancestry in unrelated individuals. Genome Res. 2009;19(9):1655–64. https://doi.org/10.1101/gr.094052.109.
21. Yang JA, Lee SH, Goddard ME, Visscher PM. GCTA: A tool for genome-wide complex trait analysis. Am J Hum Genet. 2011;88(1):76–82. https://doi.org/10.1016/j.ajhg.2010.11.011.
22. Zhang C, Dong SS, Xu JY, He WM, Yang TL. PopLDdecay: A fast and effective tool for linkage disequilibrium decay analysis based on variant call format files. Bioinformatics. 2019;35(10):1786–8. https://doi.org/10.1093/bioinformatics/bty875.
23. Zhou X, Stephens M. Genome-wide efficient mixed-model analysis for association studies. Nat Genet. 2012;44(7):821–4. https://doi.org/10.1038/ng.2310.
24. Elango D, Wang WY, Thudi M, Sebastiar S, Ramadoss BR, Varshney RK. Genome-wide association mapping of seed oligosaccharides in chickpea. Front Plant Sci. 2022;13:1024543.

https://doi.org/10.3389/fpls.2022.1024543.

25. Li MJ, Yu Q, Wei JW, Li XB, Hao AJ, Liu F, et al. Genome-wide characterization and expression analysis of the MYB transcription factor family in mung bean (*Vigna radiata*). BMC Plant Biol. 2026;26(1):766. https://doi.org/10.1186/s12870-026-08555-1.
26. Delie SM, Adamu TA, Andualem AM. Adaptability and agronomic performance evaluation of mungbean (*Vigna radiata* (L.) Wilczek) varieties under non-inoculated and inoculated rhizobium bacteria conditions. PeerJ. 2025;13:e19558. https://doi.org/10.7717/peerj.19558.
27. Ryu H, Laffont C, Frugier F, Hwang I. MAP kinase-mediated negative regulation of symbiotic nodule formation in *Medicago truncatula*. Mol Cells. 2017;40(1):17–23. https://doi.org/10.14348/molcells.2017.2211.
28. Liu H, Zhang C, Yang J, Yu N, Wang ET. Hormone modulation of legume-rhizobial symbiosis. J Integr Plant Biol. 2018;60(8):632–48. https://doi.org/10.1111/jipb.12653.
29. Kirolinko C, Yacullo M, Blanco F, Zanetti ME. Hormone-modulated transcription factors orchestrating the root nodule symbiosis. Front Plant Sci. 2026;17:1811506. https://doi.org/10.3389/fpls.2026.1811506.
30. Ke XL, Xiao H, Peng YQ, Wang J, Lv Q, Wang XL. Phosphoenolpyruvate reallocation links nitrogen fixation rates to root nodule energy state. Science. 2022;378(6623):971–7. https://doi.org/10.1126/science.abq8591.
31. Wang P, Jiang F, Xue ZH, Bu FJ, Zhu WQ, Zhang YX, et al. The *Medicago* SPX1/3-PHR2 network relays phosphate signaling to orchestrate root nodulation-dependent nitrogen acquisition by controlling flavonoid biosynthesis. Plant Commun. 2026;7(4):101695. https://doi.org/10.1016/j.xplc.2026.101695.
32. Chen JS, Xu HF, Liu QL, Ke MY, Zhang ZQ, Wang X, et al. Shoot-to-root communication via GmUVR8-GmSTF3 photosignaling and flavonoid biosynthesis fine-tunes soybean nodulation under UV-B light. New Phytol. 2024;241(1):209–26. https://doi.org/https://doi.org/10.1111/nph.19353.
33. Shen YR, Yan Y, Yin T, Zhang HY, Zhu HJ, Zhang SY, et al. An isoflavone reductase-like protein MtIFL negatively regulates nodule symbiosis in *Medicago truncatula*. New Phytol. 2025;247(3):1352–69. https://doi.org/10.1111/nph.70251.
34. Libault M, Joshi T, Takahashi K, Hurley-Sommer A, Puricelli K, Blake S, et al. Large-scale analysis of putative soybean regulatory gene expression identifies a *Myb* gene involved in soybean nodule development. Plant Physiol. 2009;151(3):1207–20. https://doi.org/10.1104/pp.109.144030.
35. Gao JP, Xia CJ, Chiu CH, Chen QC, Jiang SY, Wu XT, et al. An NSP2-MYB module orchestrates flavonoid biosynthesis and nodule symbiosis. Cur Biol. 2026;36(4):940–53.e5. https://doi.org/10.1016/j.cub.2026.01.013.
36. Zhu XF, Yan XF, Li WJ, Zhang MY, Leng JC, Yu QQ, et al. GmERF13 mediates salt inhibition of nodulation through interacting with GmLBD16a in soybean. Nat Commun. 2025;16(1):435. https://doi.org/10.1038/s41467-024-55495-1.

37. Wang XD, Chen K, Zhou MM, Gao YK, Huang HM, Liu C, et al. GmNAC181 promotes symbiotic nodulation and salt tolerance of nodulation by directly regulating GmNINa expression in soybean. New Phytol. 2022;236(2):656–70. https://doi.org/10.1111/nph.18343.
38. Wang LL, Tian T, Liang JJ, Li RH, Xin X, Qi YM, et al. A transcription factor of the NAC family regulates nitrate-induced legume nodule senescence. New Phytol. 2023;238(5):2113–29. https://doi.org/10.1111/nph.18896.
39. Yu HX, Xiao AF, Wu JS, Li HX, Duan Y, Chen QS, et al. GmNAC039 and GmNAC018 activate the expression of cysteine protease genes to promote soybean nodule senescence. Plant Cell. 2023;35(8):2929–51. https://doi.org/10.1093/plcell/koad129.
40. Pawela A, Banasiak J, Biala W, Martinoia E, Jasinski M. MtABCG20 is an ABA exporter influencing root morphology and seed germination of *Medicago truncatula*. Plant J. 2019;98(3):511–23. https://doi.org/10.1111/tpj.14234.
41. Jamruszka T, Banasiak J, Pawela A, Jarzyniak K, Xia J, Biała-Leonhard W, et al. MtABCG40 is a cytokinin transporter that limits lateral root density and nodule formation in *Medicago truncatula*. Plant J. 2025;124(5):e70622. https://doi.org/10.1111/tpj.70622.
42. Valkov VT, Rogato A, Alves LM, Sol S, Noguero M, Léran S, et al. The nitrate transporter family protein LjNPF8.6 controls the N-fixing nodule activity. Plant Physiol. 2017;175(3):1269–82. https://doi.org/10.1104/pp.17.01187.
43. Vittozzi Y, Nadzieja M, Rogato A, Radutoiu S, Valkov VT, Chiurazzi M. The *Lotus japonicus NPF3.1* is a nodule-induced gene that plays a positive role in nodule functioning. Front Plant Sci. 2021;12:685334. https://doi.org/10.3389/fpls.2021.688187.
44. Nishida H, Tanaka S, Handa Y, Ito M, Sakamoto Y, Matsunaga S, et al. A NIN-LIKE PROTEIN mediates nitrate-induced control of root nodule symbiosis in *Lotus japonicus*. Nat Commun. 2018;9(1):499. https://doi.org/10.1038/s41467-018-02831-x.
45. Valkov VT, Sol S, Rogato A, Chiurazzi M. The functional characterization of *LjNRT2.4* indicates a novel, positive role of nitrate for an efficient nodule N_2-fixation activity. New Phytol. 2020;228(2):682–96. https://doi.org/10.1111/nph.16728.
46. Misawa F, Ito M, Nosaki S, Nishida H, Watanabe M, Suzuki T, et al. Nitrate transport via NRT2.1 mediates NIN-LIKE PROTEIN-dependent suppression of root nodulation in *Lotus japonicus*. Plant Cell. 2022;34(5):1844–62. https://doi.org/10.1093/plcell/koac046.
47. Xie F, Murray JD, Kim J, Heckmann AB, Edwards A, Oldroyd GED, et al. Legume pectate lyase required for root infection by rhizobia. Proc Natl Acad Sci U S A. 2012;109(2):633–8. https://doi.org/10.1073/pnas.1113992109.
48. Zhang X, Chen JX, Lian WT, Zhou HW, He Y, Li XX, et al. Molecular module GmPTF1a/b-GmNPLa regulates rhizobia infection and nodule formation in soybean. New Phytol. 2024;241(4):1813–28. https://doi.org/10.1111/nph.19462.
49. Li N, Lin Z, Yu PY, Zeng YL, Du SX, Huang LJ. The multifarious role of callose and callose synthase in plant development and environment interactions. Front Plant Sci. 2023;14 1183402.

https://doi.org/10.3389/fpls.2023.1183402.

50. Minguillón S, Matamoros MA, Duanmu D, Becana M. Signaling by reactive molecules and antioxidants in legume nodules. New Phytol. 2022;236(3):815–32. https://doi.org/10.1111/nph.18434.

Figures

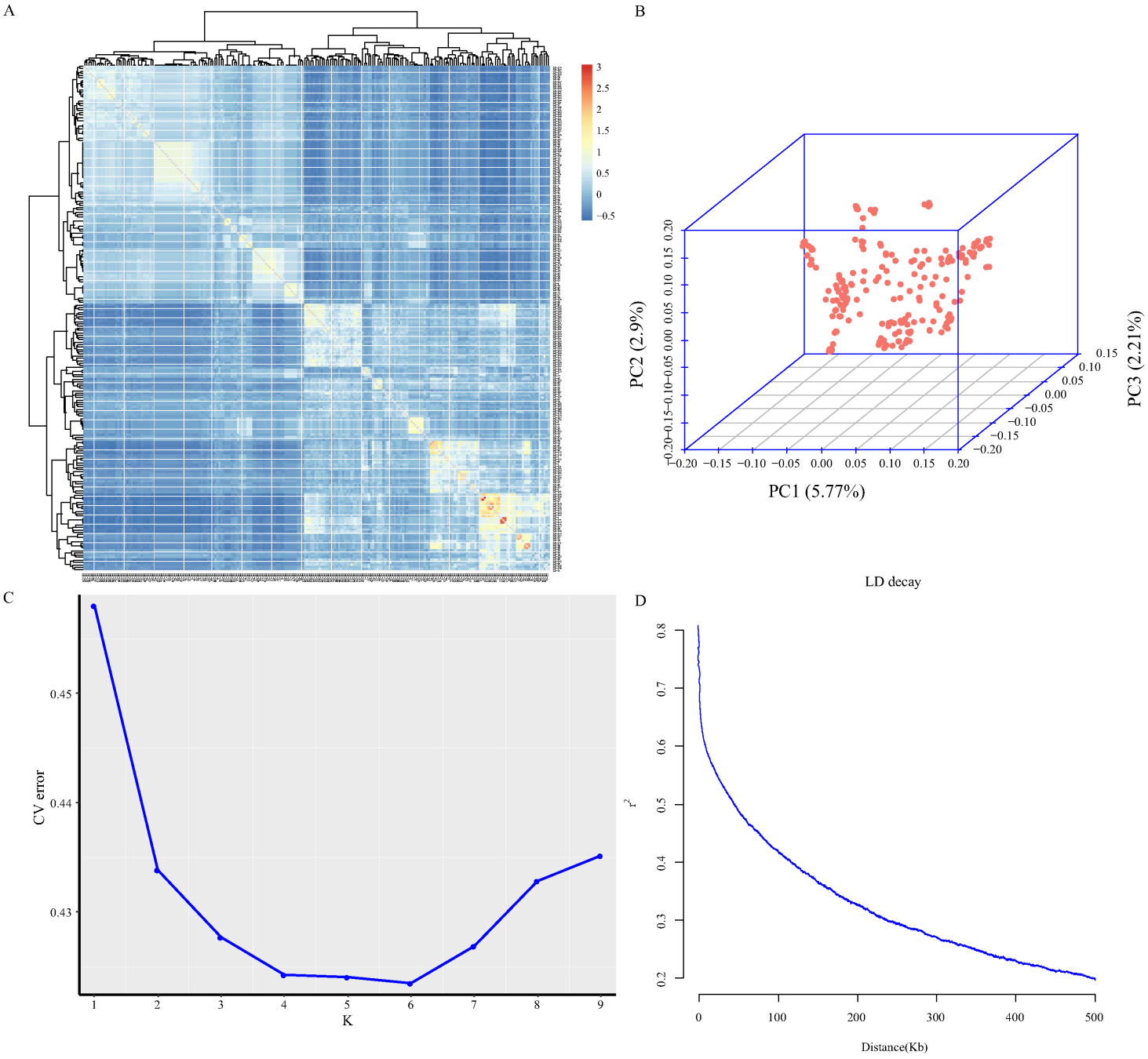


Figure 1

Population structure and linkage disequilibrium (LD) decay analysis of the association panel comprising 218 mung bean genotypes. (a) Heatmap of the genetic relationships among the 218 mung bean genotypes. (b) Principal component analysis (PCA) of the 218 mung bean genotypes. (c) Cross-validation error values for different numbers of genetic clusters (K = 1–10) based on genotype data. (d) LD decay analysis of the 218 mung bean genotypes.

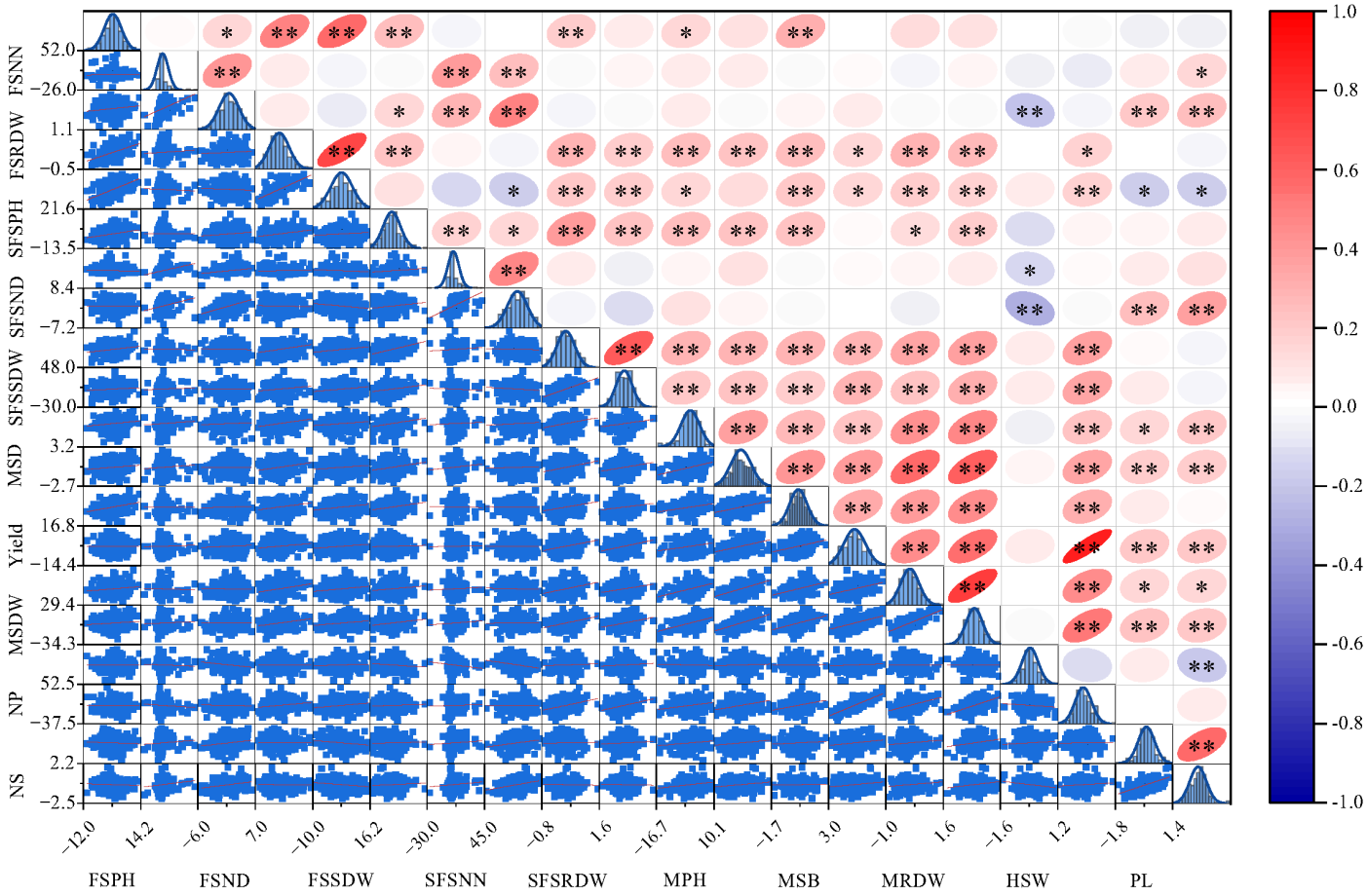


Figure 2

Frequency distributions and correlation analysis of 20 phenotypic response traits. Frequency distribution histograms for the 20 traits are shown along the diagonal, scatter plots between trait pairs are shown below the diagonal, and correlation coefficients are shown above the diagonal. Significant correlations are indicated by ** and * at $P < 0.01$ and $P < 0.05$, respectively.

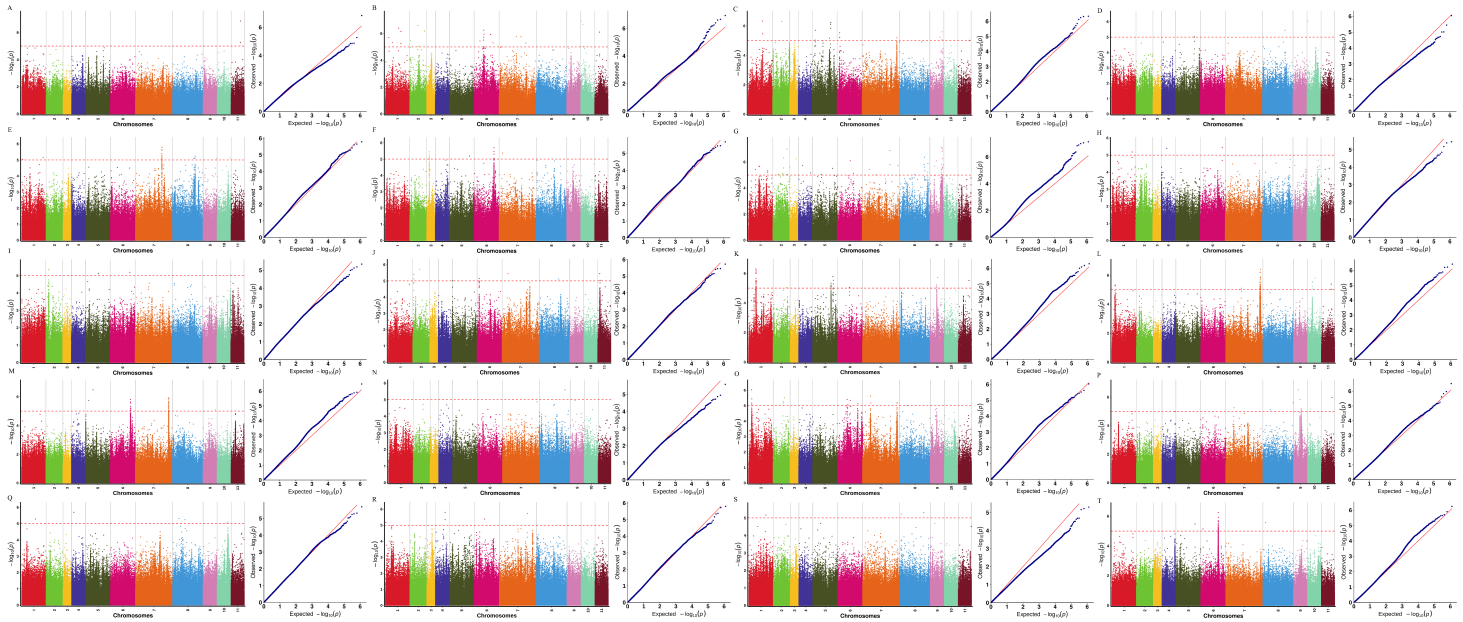


Figure 3

Manhattan and quantile–quantile (Q–Q) plots of GWAS for 20 phenotypic response traits in 218 mung bean genotypes. At the flowering stage, plant height (FSPH), stem dry weight (FSSDW), root dry weight (FSRDW), nodule number (FSNN), and maximum nodule diameter (FSND) were measured. At the seed-filling stage, plant height (SFSPH), stem dry weight (SFSSDW), root dry weight (SFSRDW), nodule number (SFSNN), and maximum nodule diameter (SFSND) were measured. At maturity, plant height (MPH), main stem diameter (MSD), number of stem branches (MSB), stem dry weight (MSDW), root dry weight (MRDW), pod number per plant (NP), seed number per plant (NS), length of the pod (PL), 100-seed weight (HSW), and yield per plant were measured.

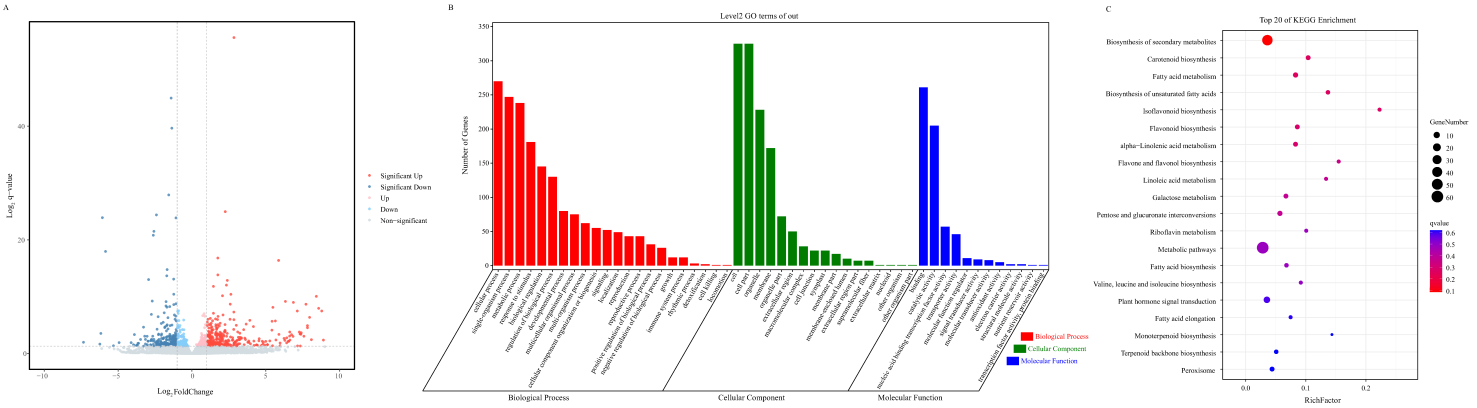


Figure 4

RNA-seq analysis of the contrasting mung bean genotypes LD55 and LD164. (a) Volcano plot showing differentially expressed genes between LD55 and LD164. (b) Gene Ontology (GO) enrichment analysis of differentially expressed genes. (c) Kyoto Encyclopedia of Genes and Genomes (KEGG) pathway enrichment analysis of differentially expressed genes.

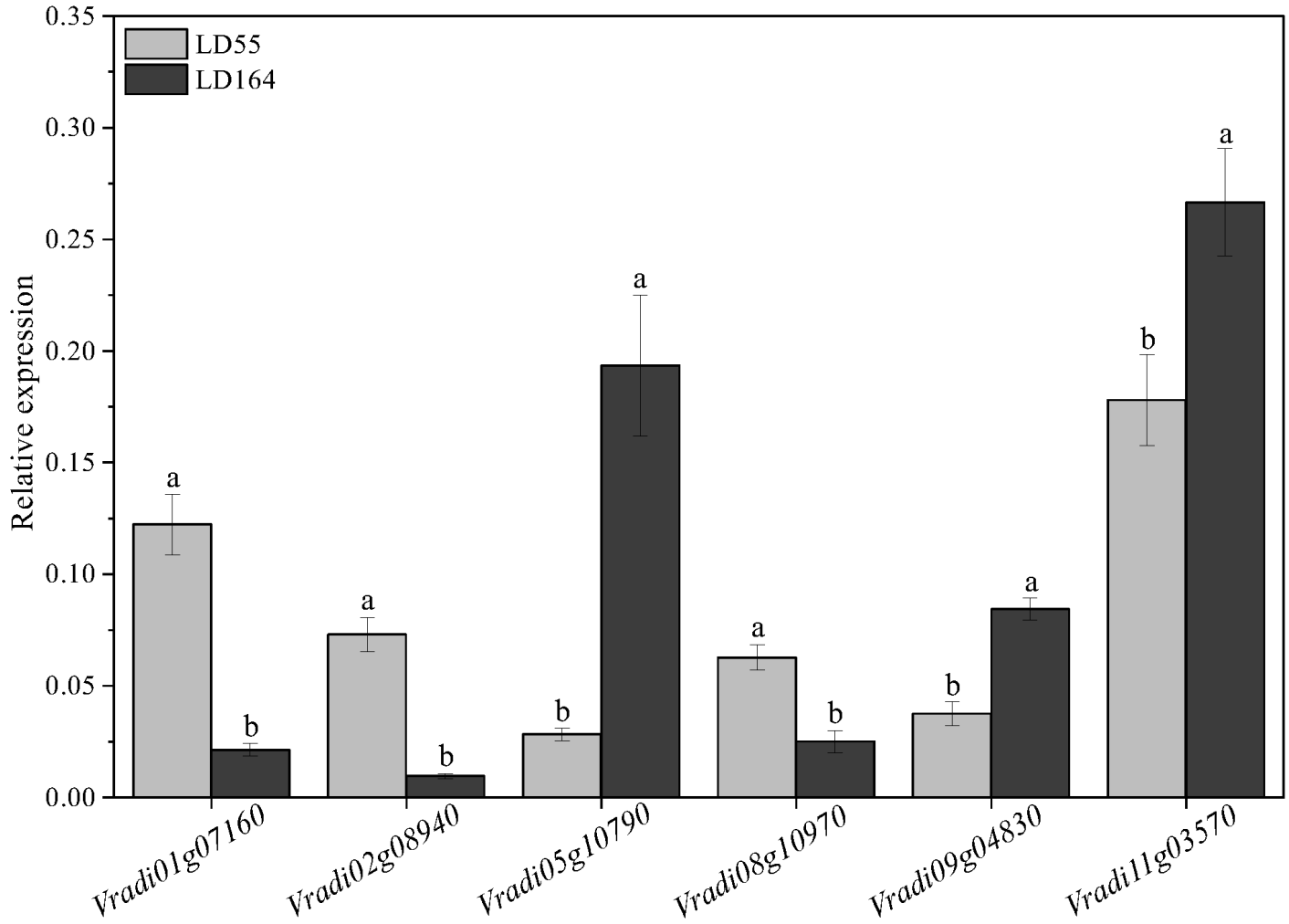


Figure 5

Quantitative real-time PCR (qPCR) validation of candidate genes identified through integrated GWAS and RNA-seq analysis. Bars represent mean ± standard error (SE) from three biological replicates (n = 3).

Supplementary Files

This is a list of supplementary files associated with this preprint. Click to download.

- Supplementtables.xlsx
- FS2.pdf
- FS1.pdf